ELSEVIER

Surface Science 454–456 (2000) 101–105

surface science

www.elsevier.nl/locate/susc

Study of the adsorption structure of NO on Pt(111) by scanning tunneling microscopy and high-resolution electron energy-loss spectroscopy

Masuaki Matsumoto [a,*], Katsuyuki Fukutani [a], Tatsuo Okano [a], Kouji Miyake [b], Hidemi Shigekawa [b], Hiroyuki Kato [c], Hiroshi Okuyama [c], Maki Kawai [c]

[a] *Institute of Industrial Science, University of Tokyo, Megro-ku, Tokyo 153-8505, Japan*
[b] *Institute of Applied Physics, CREST, Japan Science and Technology Corporation (JST), University of Tsukuba, Tsukuba 305-8573, Japan*
[c] *RIKEN (The Institute of Physical and Chemical Research), 2-1 Hirosawa, Wako, Saitama 351-0198, Japan*

Abstract

The structure of nitric oxide (NO) on a Pt(111) surface was studied by scanning tunneling microscopy (STM) and high-resolution electron energy-loss spectroscopy (HREELS). The coexistence of two species is observed by STM after saturating the surface with NO at 70 K and annealing to 215 K. Two pairs of N—O and Pt—N stretching vibrational frequencies are observed in HREELS spectra after annealing, which are assigned to the two species observed by STM. Comparison between the spectra of HREELS and infrared absorption spectroscopy (IRAS) indicates that IRAS is less sensitive to the lower-frequency mode. A new model for the adsorption structure of NO on the Pt(111) surface is proposed and discussed.

Keywords: Chemisorption; Electron energy loss spectroscopy (EELS); Electron stimulated desorption (ESD); Nitrogen oxides; Platinum; Scanning tunneling microscopy; Surface structure, morphology, roughness, and topography; Vibrations of adsorbed molecules

1. Introduction

The vibrational modes of an adsorbate are closely related to its adsorption structure on the surface. Therefore, vibrational spectra measured by high-resolution electron energy-loss spectroscopy (HREELS) or infrared absorption spectroscopy (IRAS) are utilized for structure determination of adsorbates. However, structure determination on the basis of vibrational data is sometimes misleading. Additional information obtained by other techniques such as thermal desorption spectroscopy (TDS), low-energy electron diffraction (LEED) or scanning tunneling microscopy (STM) are indispensable to determine the structure correctly. The structure of NO on Pt(111) is one of the cases that has not yet been clarified successfully on the basis of vibrational studies [1–11].

NO adsorbs molecularly on the Pt(111) surface at low temperatures (80–160 K). In the vibrational spectra [1–4], an N—O stretching vibrational mode is observed at 1490 cm^{-1} at low coverages. As the coverage increases, a new vibrational mode appears at 1710 cm^{-1}. On the basis of this meas-

* Corresponding author. Fax: +81-3-5452-6132.
E-mail address: masuaki@iis.u-tokyo.ac.jp (M. Matsumoto)

0039-6028/00/$ - see front matter
PII: S0039-6028(00)00266-1

urement, Gland and Sexton proposed a model in which NO first adsorbs on the bridge site and transits to the on-top site with increasing coverage [2]. This model has been supported to date [4–7,12] in spite of several inconsistencies. The mode at 1490 cm^{-1} that was assigned to NO on the bridge site disappears only in IRAS spectra [4] but remains with reasonable intensity in HREELS spectra up to saturation coverage [1,2]. A large desorption peak of molecular NO is observed at about 200 K by TDS. However, the origin of this peak is not well understood because no significant change has been observed in the vibrational spectra after annealing to 260 K [2,4]. The saturation coverage was determined to be 0.54 monolayers (1 ML = 1.5×10^{15} cm^{-2}) by X-ray photoelectron spectroscopy (XPS) [8]. This value is much larger than the value of 0.25 ML in Gland and Sexton's model. In our previous report, two different species were observed and assigned to the two modes observed in the vibrational spectra [9]. However, as the surface temperature in the measurements in Ref. [9] was lower than the condensation temperature (80 K) of NO, three-dimensional growth occurred before completion of the 2×2 layer. In addition, these results could not be compared directly with the results of the vibrational studies [1,2,4], which were performed at higher temperatures (90–160 K). Hence, in this work, the adsorption structure after annealing above 200 K was studied by using STM and HREELS. Annealing is useful to construct a well-ordered 2×2 structure and reveals the coexistence structure of two NO species at high coverages. The effect of annealing on the HREELS spectra and the comparison with IRAS spectra are discussed qualitatively.

2. Experimental

The STM and HREELS experiments were carried out in two separate ultrahigh vacuum (UHV) chambers. The STM chamber [9] and the HREELS chamber [13] have been described in detail elsewhere. The measurements and exposure to NO were carried out at about 70 K (STM) and 90 K (HREELS). Each Pt(111) sample was cleaned by repeated cycles of Ar^+-ion sputtering and annealing at 1400 K, and by repeated cycles of annealing under 2×10^{-5} Pa of oxygen at 1100 K and flashing to 1400 K. The cleanliness of the sample was checked by STM or HREELS. After cleaning, each sample was exposed to NO up to saturation. The surface was then annealed to 200–250 K and cooled again to the respective measurement temperature. A molecular desorption of NO is observed at 190 K, and no other molecular desorption is observed in the temperature region between 200 and 270 K in TDS spectra [2,4]. The species that desorb at 190 K can be removed by keeping the sample at 200 K for several seconds. The reproducibility of the construction of a well-ordered 2×2 structure by annealing was confirmed by STM. Therefore, the adsorption structure of NO in the STM and HREELS experiments is identical after annealing to 200–250 K.

3. Results and discussion

A topographic STM image of NO/Pt(111) measured at 70 K after annealing to 215 K is shown in Fig. 1a ($V_{sample} = -0.1$ V, $I_{tunnel} = 0.5$ nA, 7.6 nm × 7.6 nm). A well-ordered 2×2 structure is observed on the surface. It is noticed that the upper triangle in the unit cell is darker than the lower one, suggesting that the two different NO species denoted by α and β are present on the surface. The β species appears to be higher than the α species. This is shown more clearly in Fig. 1b ($V_{sample} = -0.1$ V, $I_{tunnel} = 0.5$ nA, 5.7 nm × 5.7 nm), which was measured after electron irradiation: after the measurement of Fig. 1a, the feedback loop of the STM was briefly turned off and a voltage pulse (−2 V, 100 ms) was applied to the STM tip. This caused partial desorption of NO molecules. The mechanism of this electron-stimulated desorption will be discussed elsewhere [14]. Since the electron irradiation was conducted in the area on the right side of Fig. 1b, only the molecules in the right half ('A') were affected. In this area, most of the β species are desorbed but the α species remain on the surface. In contrast, both species (α and β) can be observed in region 'B'. The two

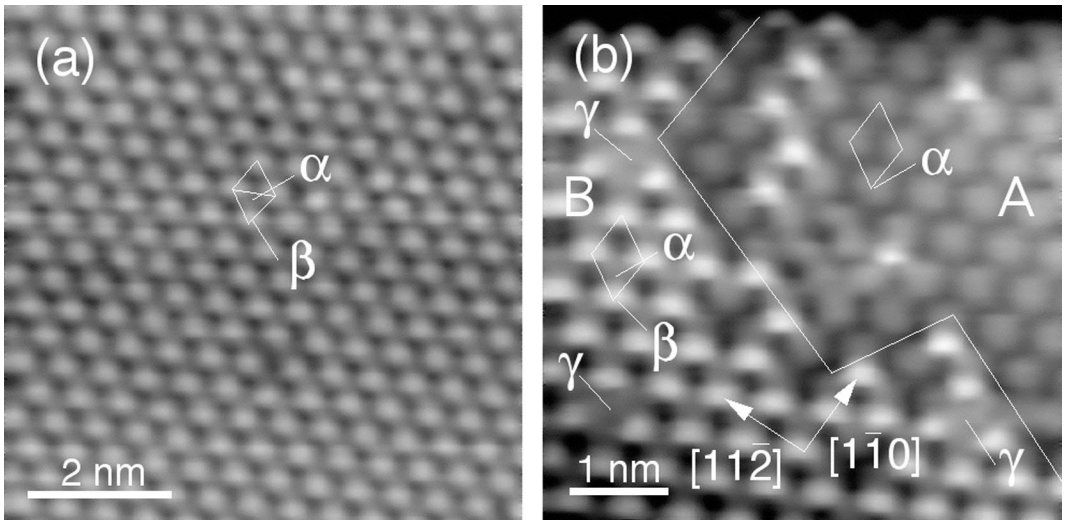

Fig. 1. (a) Topographic STM image of NO on Pt(111) after annealing to 215 K. A well-ordered 2×2 structure is constructed on the surface. Two species (α and β) appearing at different heights are present on the surface. (b) Magnified image of the same area as (a) after electron irradiation from the STM tip. Most of the β species in the region 'A' are desorbed by the electron irradiation. Several unit cells indicated by γ are bright in the whole area.

species both construct 2×2 structures, with the β species being located on the three-fold hollow site of the α species. The heights of the α and β species are 0.05 and 0.09 nm, respectively, which are the same as the values of the two species described in our previous STM report [9]. As the geometric structures are also identical in both measurements, the α and β species in Fig. 1a are identical to the 'lower' and 'higher' species in Ref. [9]. While the presence of the coexistence structure was attributed to the low measurement temperature in Ref. [9], Figs. 1a and b clearly show that the coexistence structure still remains at temperatures above 200 K. The NO coverage estimated from Fig. 1a is 0.5 ML.

HREELS spectra of NO on Pt(111) measured at 90 K are shown in Fig. 2. All spectra were measured at an incident angle of 60° in a specular reflection. The azimuthal direction and the energy of the incident electrons were [$\bar{2}$11] and 7.1 eV, respectively. At low coverages (Fig. 2a), two loss peaks are observed at 330 ($\nu_{Pt-N(a)}$) and 1484 ($\nu_{NO(a)}$) cm^{-1}, which can be assigned to the stretching vibrations of Pt—N (ν_{Pt-N}) and N—O (ν_{NO}), respectively. At saturation coverage (Fig. 2b), two ν_{Pt-N} modes are observed at 290 ($\nu'_{Pt-N(a)}$) and

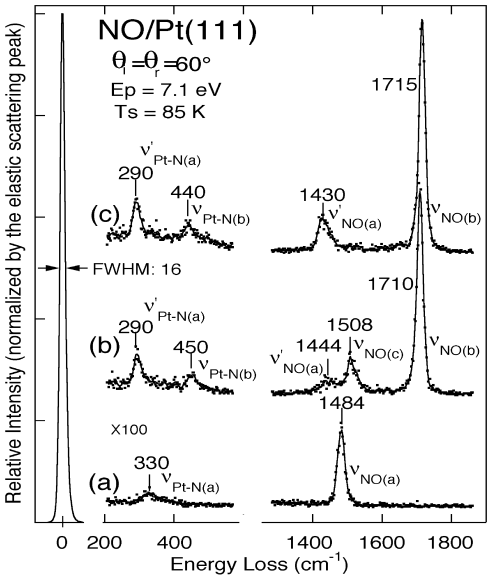

Fig. 2. HREELS spectra of NO on Pt(111): (a) at low coverages at 90 K, (b) at saturation coverage at 90 K and (c) after annealing to 200 K.

450 ($\nu_{Pt-N(b)}$) cm^{-1} and three ν_{NO} modes appear at 1444 ($\nu'_{NO(a)}$), 1508 ($\nu_{NO(c)}$) and 1710 ($\nu_{NO(b)}$) cm^{-1}. The features agree well with previous EELS spectra

[1,2] but $\nu'_{NO(a)}$ and $\nu_{NO(c)}$ are well resolved in our spectrum by virtue of higher energy resolution and sensitivity. After annealing to 200 K (Fig. 2c), $\nu_{NO(c)}$ disappears and small shifts of the other modes are observed. The presence of two pairs of ν_{Pt-N} and ν_{NO} is consistent with the finding of two species in the STM images of Fig. 1. According to the coverage dependence of the STM image, $\nu_{NO(a)}$ and $\nu_{NO(b)}$ were assigned to the 'lower' and 'higher' species in Fig. 3 of Ref. [9], because the 'lower' species was noticed at low coverages before the 'higher' species appeared. As both species are present after annealing, $\nu'_{NO(a)}$ and $\nu_{NO(b)}$ can be assigned to the α and the β species in Fig. 1b, respectively. It is suggested that the ν_{NO} mode of the α species shifts from 1484 cm^{-1} ($\nu_{NO(a)}$) to 1444 cm^{-1} ($\nu'_{NO(a)}$) by co-adsorption of the β species at high coverages.

The relative integrated intensity of $I_{\nu'_{NO(a)}}/I_{\nu_{NO(b)}}$ in Fig. 2c is 0.25. This is much smaller than the value of 1 expected from the site occupancy deduced by STM. The attenuation of the lower-frequency band was also observed in IRAS and explained by an 'intensity transfer' induced by dynamic dipole–dipole coupling in the case of densely packed adlayers of CO on Pt(111) [15,16]. A similar attenuation mechanism was suggested for the IRAS spectra of NO on Pt(111) [17]. It is therefore suggested that the growth of $\nu_{NO(b)}$ at high coverages causes the attenuation of $\nu'_{NO(a)}$, and the growth of $\nu_{NO(c)}$ causes further attenuation of $\nu'_{NO(a)}$ below the detection limit of IRAS. This is consistent with the observation that annealing causes desorption of the $\nu_{NO(c)}$ species and increases the intensity of the $\nu'_{NO(a)}$ mode. Because there are scattering processes other than dipole scattering in HREELS, e.g., impact scattering, the effect of the 'intensity transfer' is considered to be smaller than in IRAS and thus the lower-frequency mode remains observable in HREELS. This result shows that the loss of peaks in IRAS does not always indicate the loss of the vibrational mode, and great care has to be taken in the analysis of IRAS spectra.

Concerning the adsorption structure, the coverage estimated above and the azimuthal direction confirmed by the Laue method restrict the possible combinations of site occupations to the two candidates shown in Figs. 3a and b. One combination is face-centered-cubic (fcc) hollow and on-top (Model a, Fig. 3a), and another one is hexagonal close-packed (hcp) hollow and fcc hollow (Model b, Fig. 3b) for the α and β species, respectively. Ge and King showed that the fcc hollow site is the most stable adsorption site on the bare Pt(111) surface [10]. This suggests that the adsorption site populated first is the fcc hollow site. Since the coordination number is closely related to ν_{NO}, the large difference between $\nu_{NO(b)}$ and $\nu'_{NO(a)}$ is inconsistent with Model b. Furthermore, previous LEED analysis showed that NO adsorbs at the fcc hollow site at a coverage of 0.25 ML [11]. Among the two possible combinations, therefore, Model a is the most probable structure at 0.5 ML.

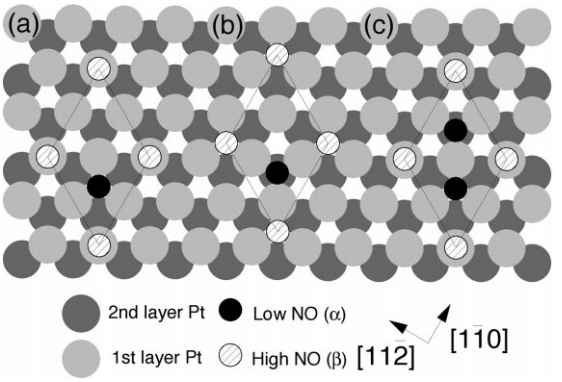

Fig. 3. Models for the adsorption structure of NO on Pt(111) showing different combinations of site occupations: (a) face-centered cubic (fcc) hollow + on-top model ($\theta = 0.5$ ML); (b) hexagonal close-packed (hcp) hollow + fcc hollow model ($\theta = 0.5$ ML); and (c) three-site model (fcc hollow + on-top + hcp hollow) for saturation coverage ($\theta = 0.75$ ML).

Assuming that the NO coverage is 0.5 ML for the sample after annealing, the saturation coverage at 90 K is estimated to be 0.74 ML by comparing the intensity of corresponding TDS spectra. This value is larger than the value of 0.54 ML obtained by Kiskinova et al. [8], which is based on the assumption that the saturation coverage of CO/Pt(111) is 0.6. However, their value agrees better with our result if one considers that the saturation coverage of CO is actually 0.67–0.71 [18–20].

At saturation coverage, an additional $\nu_{NO(c)}$ mode appears at 1508 cm^{-1} in the HREELS

spectrum in Fig. 2b. The small frequency difference between $\nu'_{NO(a)}$ and $\nu_{NO(c)}$, as well as the saturation coverage of 0.74 ML, suggest that an additional species adsorbs probably on the hcp hollow site, the model of which (Model c) is shown in Fig. 3c. The ν_{Pt-N} for this species is not observed by HREELS probably because the mode is very close to the $\nu'_{Pt-N(a)}$ mode and cannot be resolved well. The bright image in the whole unit cell at the defects indicated by γ in Fig. 1b also suggests the presence of a species on the hcp hollow site. A similar three-site occupation model has recently been reported for the adsorption of NO on Rh(111) [21,22], Pd(111) [22] and Ru(001) [23]. Therefore, this kind of structure will be a common feature of NO adsorption on transition metal surfaces. The disappearance of the $\nu_{NO(c)}$ mode after annealing shows that desorption of the molecules on the hcp hollow site is the origin of the peak at 190 K in TDS spectra [2,4].

This three-site model offers an unambiguous assignment for the site selectivity observed in the photoinduced processes of NO on Pt(111). The dissociation of NO was observed at low coverages, while molecular desorption was observed at high coverages by laser irradiation at 193 nm [7]. Furthermore, the rotational distribution of the desorbed NO was dependent on the sample temperature: the rotational distribution was Boltzmann with a rotational temperature of 500 K at saturation coverage at 90 K, and non-Boltzmann with a spin–orbit state inversion after annealing to 220 K [12,24]. Our three-site model indicates that NO adsorbed on the fcc hollow site is decomposed into atomic nitrogen and oxygen, and NO on the on-top and the hcp hollow sites is molecularly desorbed by laser irradiation with non-Boltzmann and Boltzmann distribution in the rotational motion, respectively.

4. Conclusions

STM images and HREELS spectra of NO on Pt(111) were measured after annealing the NO-saturated surface to 200–250 K. The coexistence of two NO species is observed by STM and each corresponds to two pairs of ν_{NO} and ν_{Pt-N} modes detectable by HREELS. Based on the STM images and the vibrational spectra, a new model for the adsorption structure of NO/Pt(111) is proposed.

Acknowledgements

This work was supported by the Shigekawa Project of TARA, University of Tsukuba. The support of a Grant-in-Aid for Scientific Research and Creative Basic Research from the Ministry of Education, Science, Sports and Culture of Japan is also acknowledged.

References

[1] H. Ibach, S. Lehwald, Surf. Sci. 76 (1978) 1.
[2] J.L. Gland, B.A. Sexton, Surf. Sci. 94 (1980) 355.
[3] D.S. Dunn, M.W. Severson, J.L. Hylden, J. Overend, J. Catal. 78 (1982) 225.
[4] B.E. Hayden, Surf. Sci. 131 (1983) 419.
[5] V.K. Agrawal, M. Trenary, Surf. Sci. 259 (1991) 116.
[6] J. Yoshinobu, M. Kawai, Chem. Lett. 1995 (1995) 605.
[7] M.-B. Song, M. Suguri, K. Fukutani, F. Komori, Y. Murata, Appl. Surf. Sci. 79/80 (1994) 25.
[8] M. Kiskinova, G. Pirug, H.P. Bonzel, Surf. Sci. 136 (1984) 285.
[9] M. Matsumoto, N. Tatsumi, K. Fukutani, T. Okano, T. Yamada, K. Miyake, K. Hata, H. Shigekawa, J. Vac. Sci. Technol. A 17 (1999) 1577.
[10] Q. Ge, D.A. King, Chem. Phys. Lett. 285 (1998) 15.
[11] N. Materer, A. Barbieri, D. Gardin, U. Starke, J.D. Batteas, M.A. VanHove, G.A. Somorjai, Surf. Sci. 303 (1994) 319.
[12] K. Fukutani, Y. Murata, R. Schwarzwald, T.J. Chuang, Surf. Sci. 311 (1994) 247.
[13] H. Kato, J. Yoshinobu, M. Kawai, Surf. Sci. 427–428 (1999) 69.
[14] M. Matsumoto, K. Fukutani, T. Okano, T. Yamada, M. Miyake, H. Shigekawa, in preparation.
[15] M.W. Severson, C. Stuhlmann, I. Villegas, M.J. Weaver, J. Chem. Phys. 103 (1995) 9832.
[16] I. Villegas, M.J. Weaver, J. Chem. Phys. 101 (1994) 1648.
[17] I. Villegas, R. Gómez, M.J. Weaver, J. Phys. Chem. 99 (1995) 14 832.
[18] G. Ertl, M. Neumann, K.M. Streit, Surf. Sci. 64 (1977) 393.
[19] N.R. Avery, J. Chem. Phys. 74 (1981) 4202.
[20] B.N.J. Persson, M. Tüshaus, A.M. Bradshaw, J. Chem. Phys. 92 (1990) 5034.
[21] I. Zasada, M.A. VanHove, G.A. Somorjai, Surf. Sci. Lett. 418 (1998) L89.
[22] D. Loffreda, D. Simon, P. Sautet, Chem. Phys. Lett. 291 (1998) 15.
[23] M. Stichler, D. Menzel, Surf. Sci. 391 (1997) 47.
[24] S.A. Buntin, L.J. Richter, D.S. King, R.R. Cavanagh, J. Chem. Phys. 91 (1989) 6429.